Environmental Science & Technology

Article

pubs.acs.org/est

Enhanced Partitioning and Transport of Phenolic Micropollutants within Polyamide Composite Membranes

Emil Drazevic,[†] Sarit Bason,[‡] Kresimir Kosutic,[†] and Viatcheslav Freger*,[§]

[†]Faculty of Chemical Engineering and Technology, University of Zagreb, Marulicev trg 19, 10000 Zagreb, Croatia
[‡]Zuckerbeg Institute for Water Research, Ben-Gurion University of the Negev, Sde-Boqer 84990, Israel
[§]The Wolfson Department of Chemical Engineering, Technion − Israel Institute of Technology, Haifa 32000, Israel

ABSTRACT: Aromatic phenols represent an important class of endocrine-disrupting and toxic pollutants, many of which (e.g., bisphenol A and substituted phenols) are known to be insufficiently removed by reverse osmosis (RO) and nanofiltration polyamide membranes that are widely used for water purification. In this study, the mechanism of phenol transport across the polyamide layer of RO membranes is studied using model phenolic compounds hydroquinone (HQ) and its oxidized counterpart benzoquinone (BQ). The study employs filtration experiments and two electrochemical techniques, impedance spectroscopy (EIS) and chronoamperometry (CA), to evaluate the permeability of an RO membrane SWC1 to these solutes in the concentration range 0.1−10 mM. In addition, combination of the permeability data with EIS results allows separately estimating the average diffusivity and partitioning of BQ and HQ. All methods produced permeability of the order 10^{-7} to 10^{-6} m s^{-1} that decreased with solute concentration, even though the permeability obtained from filtration was consistently lower. The decrease of permeability with concentration could be related to the nonlinear convex partitioning isotherm, in agreement with earlier measurements by FTIR. The diffusivity of HQ and BQ was estimated to be of the order 10^{-15} m^2 s^{-1} and partitioning coefficient of the order 10. The high affinity of phenols toward polyamide and their high uptake may change membrane characteristics at high concentration of the solute. EIS results and hydraulic permeability indeed showed that permeability to ions and water significantly decreases with increasing concentration of organic solute.

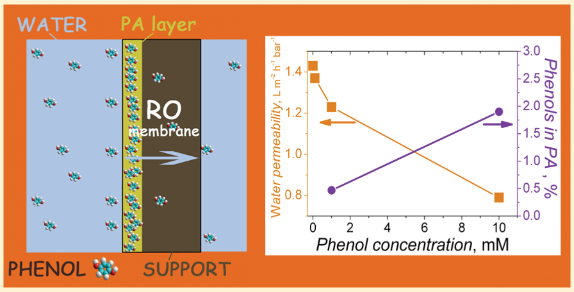

INTRODUCTION

Reverse osmosis (RO) and nanofiltration (NF) membranes are widely used in water treatment, desalination, and purification. Despite their wide use, the mechanism of removal of organics, such as pharmaceuticals, hormones, pesticides, and other toxic compounds that may have an adverse effect on living organisms, is still poorly understood. It is fairly well established today that the rejection of uncharged organics by NF and RO membranes cannot be viewed as a simple sieving determined by the ratio of the solute and pore radii. Kosutic and Kunst reported that among different NF membranes the one with the smallest pores would not always have the highest rejection of the same solute.[1] On the other hand, for a given membrane and different solutes a poor correlation between rejection and the solute radius is often observed. This apparently indicates importance of physicochemical interactions and affinity between the membrane and the solute.[2]

The solute permeability is determined by both frictional and thermodynamic factors. The former are mainly size-dependent therefore the nonsteric physicochemical interactions mainly enter through thermodynamics, i.e., the partitioning of the solute between the membrane and solution.[3] Overall, the partitioning coefficient is not as much dependent on pore and solute radii as on the solute's affinity to the membrane. Recently a fairly good prediction of the rejection of various uncharged organic molecules by NF and RO membranes was achieved through incorporation of the partitioning coefficient in the transport model.[4,5] This coefficient was calculated as a product of steric exclusion coefficient[6] and a Boltzmann factor employing the free energy of interaction between the liquid solutes and membrane estimated through contact angle measurements.[7] Unfortunately, these calculations of partitioning could not be verified by direct measurements, which are formidably difficult due to the thinness of the active polyamide layer that is ∼10^3 times thinner than the supporting polysulfone film. Even though sorption measurements of some solutes by composite membranes were reported,[8,9] they did not distinguish between the sorption in the polysulfone and polyamide layers[8] or were fully dominated by the support.[9]

To separate overwhelming interferences from the support two techniques were recently proposed utilizing top polyamide films separated from genuine composite membranes and placed on a suitable solid substrate.[10−12] One method makes use of attenuated total reflection FTIR (ATR-FTIR) spectroscopy

Received: November 22, 2011
Revised: January 16, 2012
Accepted: January 18, 2012

that probes a ~1-μm thick region adjacent to a solid IR-transparent crystal with the attached polyamide film exposed to a solution. Sorption of various organics in NF and RO membranes could be quantified by measuring the intensity of specific bands of the solute, which well correlated with rejection.

The second approach, electrochemical impedance spectroscopy (EIS), utilizes a solid electrode with an attached polyamide film immersed in solution of solutes that form an electrochemical couple, i.e., can be reversibly oxidized and reduced.[11,12] This requirement of electrochemical activity of the solute is offset by the possibility to measure both partitioning and diffusion coefficients. The complex diffusion impedance measured using small AC potential perturbations in a range of frequencies may then be related to sorption and diffusion in the polyamide film.

This approach has already been used to study transport of ions and molecules in thin polymer films[12−14] and will be used here to get insight into the transport of the organic couple of aromatic diphenol hydroquinone (HQ) and its oxidized counterpart benzoquinone (BQ). As a diphenol, HQ represents an important class of pollutants, many of which (e.g., phenol, bisphenol A, and substituted phenols) are endocrine-disrupting and toxic, but insufficiently removed by reverse osmosis and nanofiltration polyamide membranes.[15−21] In addition, some phenolic compounds were found to strongly affect membrane characteristics, e.g., water permeability.[22] Even though HQ/BQ couple is among very few that suit EIS measurements, the conclusion should apply to many phenolic pollutants, which are often not so different from HQ and BQ in terms of size and affinity.

The EIS data are complemented with diffusion permeability deduced from chronoamperometry (CA) experiments, in which diffusion current is measured using the same setup as EIS under a large constant potential gradient.[10,23,24] Ultimately, the EIS and CA results are compared to the permeability deduced from regular filtration experiments. The filtration data are analyzed using a modified Spiegler−Kedem model that was recently proposed to treat such data in a model-independent way.[25] Combination of different types of data yields the most comprehensive insight into the transport of phenolic organics within polyamide membranes.

■ MATERIALS AND METHODS

Materials and Solutions. The salts, solvents, and organic solutes were of analytical grade and used as purchased. The solutions were prepared using a purified deionized water of specific resistance of 18.2 MΩ cm. Phosphate buffer (0.5 M; pH = 7) solution was prepared by mixing prescribed amounts of Na_2HPO_4 and KH_2PO_4. The membranes tested were SWC-1, CPA3, LFC1, and ESPA1 supplied as flat sheets by Hydranautics.

Electrochemical Setup, Procedures, and Analysis. The electrochemical experiments (EIS and CA) were carried out using a three-electrode cell containing about 50 cm^3 of solution (Metrohm). PEEK-shrouded GC electrodes, bare or film-covered (see above), were used as a working electrode. The preparation of free polyamide films supported on a PEEK-shrouded glassy carbon (GC) disk electrode of active area 0.07 cm^2 (Metrohm) is described elsewhere.[12,26] Briefly, the bottom nonwoven fabric layer was peeled off the composite membrane and, after mounting the remaining membrane onto the GC surface, the polysulfone support was washed away with dimethylformamide leaving a free polyamide film attached to electrode. A Pt wire was used as an auxiliary electrode and $Ag/AgCl_{(s)}$ electrode was used as a reference.[12] All measurements were carried out at ambient temperature in a Faraday cage (Princeton Applied Research). Prior to each experiment, the cell was purged with nitrogen to remove dissolved oxygen. The solutions were 0.5 M phosphate buffer containing an equimolar mixture of BQ and HQ at concentrations 0, 0.1, 1, or 10 mM each. In EIS experiments a 5 mV AC perturbation was superimposed on a predetermined open circuit (equilibrium) DC potential that was close to 0 V versus Ag/AgCl(s), as was also verified by cyclic voltammetry (CV). In CA experiments the current was measured vs time following a stepwise change of open circuit potential to either +0.3 V or −0.3 V for 30 s until an about constant current was obtained. The applied potential ensured, respectively, either complete oxidation of hydroquinone or complete reduction of benzoquinone, as was verified by CV.

The EIS spectra were fitted to an equivalent circuit (EC) using the Echem Analyst software (Gamry). General EC and its elements and their interpretation for the present case are described in detail elsewhere.[11,12] To verify and facilitate interpretation and analysis, EIS experiments were also conducted for conditions where certain elements of EC were absent.

The steady-state current I_{obs} observed in CA experiments with HQ/BQ solutions was first corrected using the formula

$$\frac{1}{I} = \frac{1}{I_{obs} - I_0} - \frac{1}{I_{bare}} \tag{1}$$

where I_{bare} is the steady-state current determined by the resistance of the unstirred layer and measured with a bare electrode in the same HQ/BQ solution as I_{obs}, and I_0 is the background steady-state current obtained with a film-covered electrode in a buffer solution without HQ/BQ. The corrected current I was then converted to permeability ω_s to a specific species (HQ for positive potential or BQ for negative ones) using the equation

$$\omega_s = \frac{I}{nFAC} \tag{2}$$

where $n = 2$ is the number of electrons transferred in HQ ↔ BQ reaction, $F = 96\,485$ C mol^{-1} is Faraday's constant, C is the concentration of either HQ (oxidation) or BQ (reduction) in solution, and A is the electrode area.

RO Experiments and Analysis. RO experiments were carried out in a cross-flow Sepa CF II cell (Sterlitech Corporation, USA) of a membrane area 0.0138 m^2 and channel dimensions 14.5 × 9.5 × 0.17 cm^3 (length × width × height). The feed from a 5-L tank was circulated through the cell at a flow rate of 3 L min^{-1} (fluid velocity 0.75 m s^{-1}) by means of a Hydracell DO3SASGSSSCA pump driven by a variable speed motor (Wanner Engineering Inc., Minneapolis, MN, USA). The feed tanks and pipes were protected from light, since BQ and HQ are photosensitive.[27] The volume flux through the membrane J_V was determined by collecting and weighing the permeate over a certain time. Temperature (25.0 ± 0.1 °C) was maintained using a thermostat and Danfoss XG10 heat exchanger. The pressure in all experiments with BQ and HQ solutions was varied in the order from the highest to the lowest pressure and then repeated in reversed order. The feed solutions were of concentrations 0.1, 1, and 10 mM of either BQ or HQ. The pH was adjusted to 7 with 0.005 mol L^{-1} NaOH or H_2SO_4. Prior to each measurement the flux was stabilized at 2.2 MPa for 2 h and thereafter RO experiments were carried out for about 5 h to ensure a steady state.

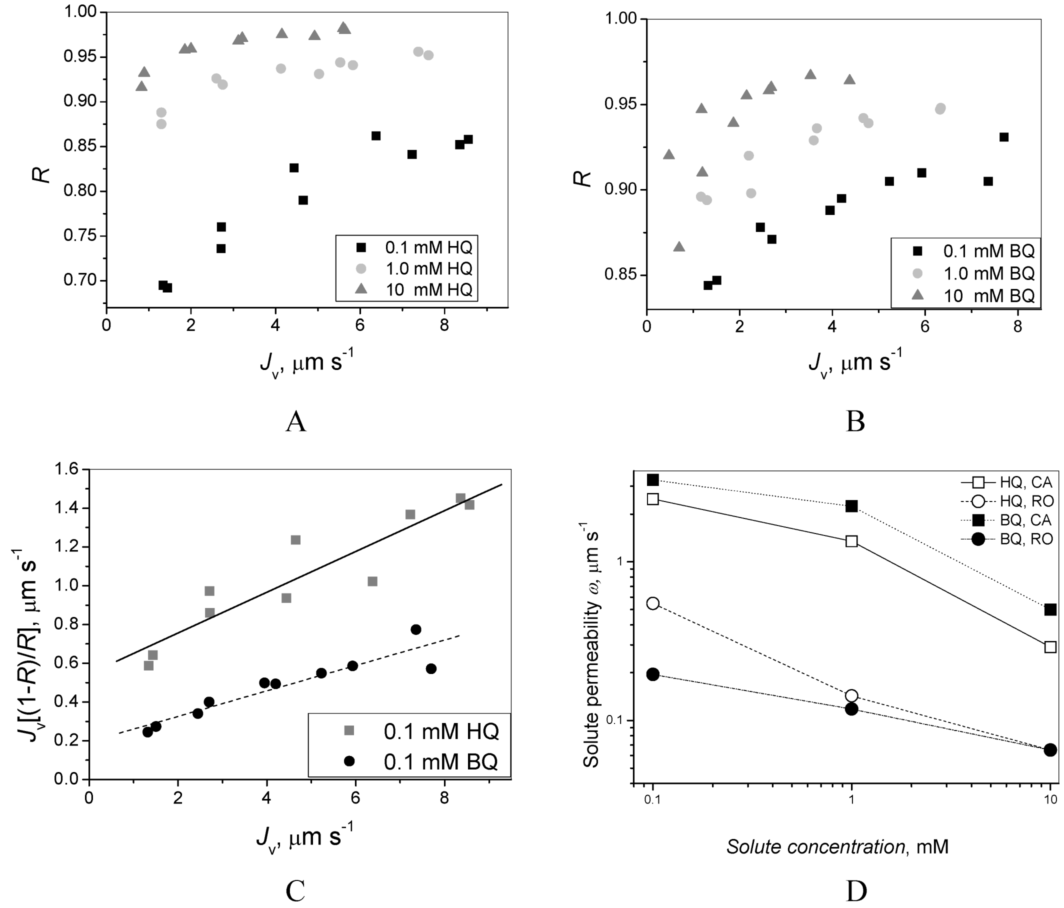

Figure 1. Observed RO rejection versus flux for feed solutions of HQ (A) and BQ (B) of three different concentrations. (C) An example of extrapolation of filtration data to zero flux for 0.1 mM BQ and HQ with intercepts yielding solute permeability; (D) HQ and BQ permeability estimates from RO and CA experiments. Lines are added for eye-guiding.

Concentrations of BQ and HQ in feed and permeate over time were determined using a Total Organic Carbon Analyzer (Shimadzu TOC V_{WS}).

The membrane permeability to solutes was evaluated from the RO data for each feed solution by extrapolating rejection data to zero flux ($J_V \to 0$) using the following solution of modified Speigler–Kedem equation[28] with concentration polarization (CP) correction

$$\begin{aligned} J_V\frac{1-R}{R} &= \frac{AJ_V}{B(1-\exp[-AJ_V])}\exp\left(\frac{J_V}{k}\right) \\ &\approx \frac{1}{B}\left(1 + J_V\left[\frac{A}{2}+k^{-1}\right]\right) \xrightarrow[J_V\to 0]{} \frac{1}{B} \approx \omega_s \end{aligned} \qquad (3)$$

where $A = (1-\sigma)/\omega_s$ and $B = \sigma/\omega_s$ are coefficients introduced previously[28] in place of permeability ω_s and reflection coefficient σ, and k is the mass transfer coefficient at upstream membrane surface. The first approximation is the linear expansion for small J_V and the last relation is suggested by the relatively high rejection at high fluxes ($\sigma \approx 1$). Regardless of the k value, both CP and concentration gradient across the membrane vanish at $J_V = 0$, therefore the extrapolated value of ω_s corresponds to the feed concentration.

RESULTS AND DISCUSSION

RO Results for Benzoquinone and Hydroquinone. Flux-rejection data obtained for SWC1 membrane and different feed solutions of BQ and HQ are shown in Figure 1A and B. Figure 1C shows typical plots of $J_V\,(1-R)/R$ versus J_V that were used for linear extrapolation to $J_V = 0$ using eq 3, which yields the value of permeability $\omega_s \approx 1/B$ at feed concentration without the need to determine the mass transfer coefficient. The resulting dependence of ω_s on the solute concentration for HQ and BQ is shown in Figure 1D. The permeability of HQ is slightly larger than that of BQ, probably due to stronger interaction of OH groups of HQ with polyamide, but the difference is fairly minor. It is seen that ω_s decreases with concentration. This behavior is different from that of most salts, which usually show ω_s increasing with salt concentration.[28] The permeability ω_s is given by

$$\omega_s = \frac{DK}{\delta} \qquad (5)$$

where D and K are, respectively, *average* solute diffusivity and partitioning within the membrane and δ is membrane thickness. D and δ usually weakly depend on concentration, then ω_s follows approximately the same dependence on concentration as K. The different concentration dependence of ω_s for HQ/BQ and salts is then explained by the shape of the sorption (partitioning) isotherm. Indeed, for salts the isotherm is often concave, as typical of Donnan exclusion, i.e., the partitioning coefficient K increases with concentration.[28] However, for organics a convex, i.e., saturating, isotherm is more typical hence K and ω_s decrease with solute concentration.[10,29] Nevertheless, RO data alone cannot show how much contribution to ω_s comes from D and K. This problem is approached in the next sections based on results of electrochemical experiments, CA and EIS.

Electrochemical Experiments (EIS and CA). EIS employs an equimolar mixture of HQ and BQ, which greatly facilitates analysis; however the obtained transport characteristics are average for two solutes. This is unlikely to affect the conclusions, since the sizes and permeabilities of the solutes are not drastically different (cf. Figure 1D). Figure 2 shows typical EIS spectra of bare and film-covered electrodes in buffer solutions with 0, 1, and 10 mM HQ/BQ. The spectra were well reproduced in at least 3 independent experiments.

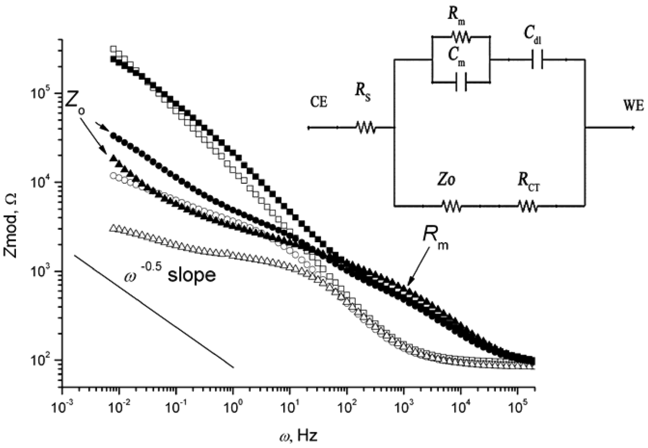

Figure 2. Representative EIS spectra (Bode plots) of SWC1 film in 0.5 M phosphate buffer containing (■,□) 0 mM HQ/BQ, (●,○) 1 mM HQ/BQ, and (▲,△) 10 mM HQ/BQ. Open and filled symbols designate bare and film-covered electrode, respectively. For clarity the phase is not shown. The inset shows the full EC used for fitting.

Two features are notable. First, for all samples, bare and film-covered, *addition of HQ/BQ couple* to buffer solution brings about a drop in impedance in the region below about 10 Hz. The drop is due to diffusion and reaction of redox species corresponding to elements Z_O and R_{ct} in EC in the lower faradaic branch of EC (inset in Figure 2). In the present context, the element of greatest interest is Z_O that appears in the spectra of HQ/BQ solutions below about 1 Hz as a line with an exponential slope −1/2 associated with diffusion of HQ and BQ across the boundary layer and/or the film covering the electrode.

Second, *addition of the film* on top of electrode is responsible for increase of impedance in 2 regions (see Figure 2):

1. around 1 kHz, which reflects membrane electrical resistance R_m associated with permeation of ions of the buffer through the film, and
2. below 1 Hz, reflecting increased resistance toward diffusion of redox organic solutes, HQ and BQ, i.e., the value of Z_O. Note that Z_O is observed for bare electrode as well (open symbols in Figure 2) due to the unstirred layer.

To resolve the transport characteristics of the film it is necessary that the diffusion impedances of the film be sufficiently larger than that of the unstirred layer. This condition was fulfilled here only for the densest SWC1 membrane and for two larger HQ/BQ concentrations, 1 and 10 mM. The reason was the slow stirring used in order to gurantee no film damage or detachment by shear stresses.

The spectra in Figure 2 are well separated from the bare electrode spectra for 1 and 10 mM and display a line with about −1/2 slope that extends down to the lowest used frequency without turning into a plateau and with a phase close to 45° (not shown). This implies that the film essentially behaves as Warburg impedance that describes diffusion in a semi-infinite film. A fit to EC circuit shown in the inset in Figure 2 yields the Warburg parameter Y_O of this element that may be related to the film characteristics and, in particular, to the quantity DK^2 as follows:[11,30]

$$DK^2 = \frac{4RTY_0}{n^2F^2CA} \tag{6}$$

where C is the total molar concentration of redox species in solution. The calculation of Y_O and DK^2 is summarized in Table 1. The values are used below to split the permeability ω_s to D and K.

The EIS setup was also used for CA experiments to independently assess the permeability along with values obtained from filtration. Typical CA runs are shown in Figure 3. It is seen that the current was reasonably close to the steady state. The permeability was then calculated using eq 2 with final value of the current corrected for parasitic background currents and resistance of unstirred layer using eq 1. Thus-calculated values of ω_s are summarized in Table 1 and Figure 1D along with the values deduced from filtration. As in EIS, the uncertainty for C = 0.1 mM was quite large due to relatively low resistance of the film compared to the unstirred layer and significant background current, however, the result is presented in Figure 1D and Table 1 as an estimate.

Combination of ω_s and Y_0 measured by CA and EIS for the same film and solution in principle allows separately evaluating D and K, provided the film thickness is known so that ω_s may be converted to the product DK. The total thickness of the polyamide layer of SWC1 was estimated to be about 100 nm, which may be viewed as an upper bound of polyamide thickness.[10,26,31] Since the active layer of RO membranes contains a significant fraction of loose polymer,[31,32] the actual barrier thickness could be smaller, even though the active layer of the SWC1 membrane is among the densest.[31] Alternative estimates were then made using a smaller value δ = 50 nm as well, viewed as a plausible lower bound. Because the value of DK^2 deduced from EIS is average of HQ and BQ, the average values of DK estimated from CA permeabilities of HQ and BQ were used as well to obtain average D and K. The results are summarized in Table 1, except for lowest concentration 0.1 mM, where the unstirred layer did not allow observing Z_O of the PA film.

Comparison of RO and CA. Figure 1D shows that the solute permeabilities ω_s deduced from RO and CA show similar trends yet the RO values are about an order of magnitude smaller. This is quite surprising, since it was shown recently that in the case of ferrocyanide salts the results by both methods were commensurate.[33] One possibility is that the support that underlies the top layer has a relatively low porosity; it was shown by simulations that this could significantly reduce observed permeability of the top layer.[34,35] The effect is purely geometric thereby it should be independent of specific solute and concentration, which seems

Table 1. Summary of Transport and Partitioning Parameters of HQ and BQ in SWC1 Membrane Deduced from RO and Electrochemical Measurements (CA and EIS)[a]

	RO		CA			EIS				
	ω_s, μm s^{-1}		ω_s, μm s^{-1}		HQ+BQ (av.)					
C, mM	HQ	BQ	HQ	BQ	$DK \times 10^{13}$, m^2 s^{-1}	$Y_O \times 10^4$, $\Omega^{-1} \times$ s$^{-1/2}$	$DK^2 \times 10^{12}$, m^2 s^{-1}	$D \times 10^{15}$, m^2 s^{-1}	K	C*, % (vol)
0. 1	0.55	0.19	4.2	5.9	2.9 (5.8)					
1	0.14	0.12	2.1	4.6	1.8 (3.6)	1.1	3.9	8.4 (2.1)	21.5 (43)	0.47 (0.95)
10	0.065	0.065	0.3	0.6	0.39 (0.78)	3.2	0.34	4.5 (1.1)	8.6 (17)	1.9 (3.8)

[a] The values of *KD*, *K*, *D*, and C* are average estimates for BQ and HQ for membrane thickness 100 nm; values for thickness 50 nm are shown in brackets. The last column shows C* as estimated volume percentage of BQ and HQ in polyamide.

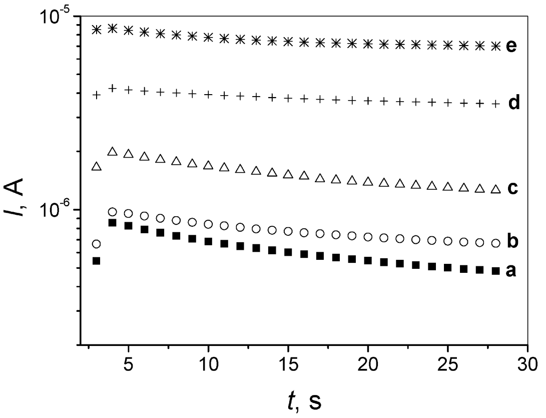

Figure 3. CA curves measured in 0.5 mM phosphate buffer: (a) bare electrode, no BQ/HQ; (b) film-covered electrode, no BQ/HQ; (c) film-covered electrode, 0.1 mM BQ/HQ; (d) film-covered electrode, 1 mM BQ/HQ; (e) film-covered electrode, 10 mM BQ/HQ. The films were isolated from SWC1 membrane. The applied potential was +0.3 V corresponding to complete oxidation of HQ.

to agree with the fairly close ratios between RO- and CA-based permeabilities throughout the analyzed range of HQ and BQ concentrations (Figure 1D). However, it is inconsistent with the results for ferrocyanides.[33]

Another plausible reason could be sorption of the solute within polysulfone support or on its inner surface.[9,36] Although in this work a long time was allowed to verify a steady-state rejection, it might not fully guarantee saturation of support. Moreover, if the sorption kinetics within the support was diffusion- rather than sorption-limited, this would result in a pseudo-steady-state rejection and the apparent permeability reduced by about the same factor for all solute concentration, as in Figure 1D. Even though the present data are insufficient to validate this mechanism, it agrees better with the results for ferrocyanide that showed no significant discrepancy between RO and CA permeabilities,[33] consistent with negligible sorption of salts in the support.

Interaction of Organic Solutes with the Active Polyamide Layer. Results in Table 1 indicate that diffusion coefficients of HQ and BQ in polyamide are small, of the order of 10^{-15} m^2 s^{-1}, i.e., about 10^6 times smaller than in water. This agrees with the fact that Stokes radii of HQ and BQ (~ 0.3 nm) are close to and may even exceed the effective average pore radius of the polyamide (about 0.2−0.3 nm).[37] In contrast, the values of *K* are very large, of the order 10, i.e., several orders of magnitude larger than corresponding values for salts,[12] indicating a strong affinity toward the membrane. Although one could expect that both sorption and diffusion should be small when the solute and pore sizes are close, the steric effect is much weaker for exclusion (sorption) than for diffusion.[6] The steric exclusion can be further weakened, if the pore size is not uniform, as typical for NF and RO membranes.[1] On the other hand, a solute closely fitting a cavity within a polymer enhances short-range molecular interactions, such as van der Waals, H-bonding etc., responsible for high affinity between the two. These findings explain the large permeability and fairly poor rejection of phenols compared to salts as well as a long time needed to achieve saturation of the PA film with organics. The large *K* values agree well with those obtained previously for HQ using ATR-FTIR method.[10]

Another notable feature mentioned earlier is dependence of *K* and ω_s on concentration (Table 1), a consequence of the nonlinear convex isotherm. Such isotherms were already observed using ATR-FTIR for HQ and other organic solutes,[10,29] even though the concentrations in those studies were higher. Curiously, the partitioning, hence permeability, decreasing with concentrations explains why the film contribution could not be observed in CA and EIS at low concentrations. Indeed, in this case the diffusion resistance of the film was lower, while that of the unstirred layer stayed constant and overwhelmed that of the film.

Based on the values of *K* it is possible to estimate the average concentration C* of HQ and BQ within polyamide, also shown in Table 1. For solution concentration 10 mM C* becomes as large as several percent, which is commensurate with the amount of water in polyamide, 5−10%.[26] Such a high fraction of organics is likely to change the properties and performance of the polyamide layer. One may expect that sorbed organics would make the film more hydrophobic, which would enhance ion exclusion and reduce film permeability to salts and water. Indeed, the value of L_p steadily decreased as the feed concentration of HQ and BQ increased in filtration experiments (Figure 4A). A direct evidence of the reduced salt permeation at increasing HQ and BQ content is found in EIS spectra, specifically, in the value of electrical resistance of the membrane R_m observed around 1 kHz in EIS (see Figure 2). Table 1 lists the values of R_m obtained for SWC1 membrane by fitting to the EC displayed in Figure 2. Whereas the diffusion impedance Z_O decreased with HQ/BQ concentration, the film resistance steadily increased from R_m = 216 Ω for clean buffer to 686 Ω at 10 mM HQ/BQ. The same trend of R_m was clearly observed for all examined RO membranes, as shown in Figure 4B. (Note that R_m could be measured for all membranes even though Z_O could only be measured for SWC1.)

Overall, the measured values of permeability, partitioning, and diffusivity indicate that affinity of phenolic permeants to polyamide RO membranes may be so strong that it may overwhelm steric exclusion. This results in a strong uptake and relatively large permeability of these solutes, despite small

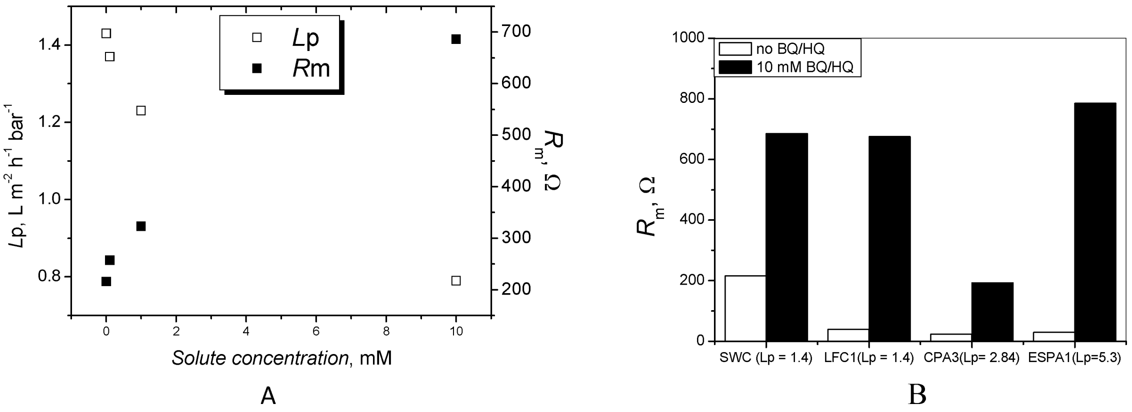

Figure 4. Effect of HQ/BQ concentration on transport properties of RO membranes. (A) Film resistances R_m and hydraulic permeability L_p of the SWC1 membrane versus HQ/BQ concentration. (B) Electrical resistance R_m of films isolated from different commercial RO membranes in 0.5 M phosphate buffer between clean buffer and 10 mM BQ/HQ.

diffusivity. Their partitioning follows a nonlinear convex isotherm thus permeability decreases and rejection increases with solute concentration, opposite to the case of salts. As a result of very high partitioning, the concentration of solute within the polyamide may become high enough to affect permeation of water and ions, as indeed observed in filtration and EIS experiments reported here.

AUTHOR INFORMATION

Corresponding Author

*E-mail: vfreger@tx.technion.ac.il.

Notes

The authors declare no competing financial interest.

ACKNOWLEDGMENTS

This work was supported by the Ministry of Science, Education and Sports of the Republic of Croatia through Project 125-1253008-3009 "Membrane and adsorption processes for removal of organic compounds in water treatment" and UKF project "Reduction of environmental risks posed by pharmaceuticals and their degradation products in process wastewaters, through RO/NF membrane treatment (REPHAD)".

REFERENCES

(1) Kosutic, K.; Kunst, B. Removal of organics from aqueous solutions by commercial RO and NF membranes of characterized porosities. *Desalination* **2002**, *142*, 47–56.

(2) Bellona, C.; Drewes, J. E.; Xu, P; Amy, G. Factors affecting the rejection of organic solutes during NF/RO treatment-a literature review. *Water Res.* **2004**, *38*, 2795–2809.

(3) Soltanieh, M.; Gill, W. N. Review of reverse osmosis membranes and transport models. *Chem. Eng. Commun.* **1981**, *12*, 279–363.

(4) Verliefde, A. R. D.; Cornelissen, E. R.; Heijmana, S. G. J.; Verberk, J. Q. J. C.; Amy, G. L.; Van der Bruggen, B.; van Dijk, J. C. J. Construction and validation of a full-scale model for rejection of organic micropollutants by NF membranes. *J. Membr. Sci.* **2009**, *339*, 10–20.

(5) Yangali-Quintanilla, V.; Verliefde, A.; Kime, T. U.; Sadmania, A.; Kennedy, M.; Amy, G. L. Artificial neural network models based on QSAR for predicting rejection of neutral organic compounds by polyamide nanofiltration and reverse osmosis membranes. *J. Membr. Sci.* **2009**, *342*, 251–262.

(6) Bowen, W. R.; Mohammad, A. W.; Hilal, N. J. Characterisation of nanofiltration membranes for predictive purposes—use of salts, uncharged solutes and atomic force microscopy. *J. Membr. Sci.* **1997**, *126*, 91.

(7) Verliefde, A. R. D.; Cornelissen, E. R.; Heijman, S. G. J.; Hoek, E. M. V.; Amy, G. L.; Van der Bruggen, B.; van Dijk, J. C. Influence of solute-membrane affinity on the rejection of uncharged organic solutes by nanofiltration membranes. *Environ. Sci. Technol.* **2009**, *43* (7), 2400.

(8) Kimura, K.; Amy, G. L.; Drewes, J.; Watanabe, Y. Adsorption of hydrophobic compounds onto NF/RO membranes: an artefact leading to overestimation of rejection. *J. Membr. Sci.* **2003**, *221*, 89–101.

(9) Schutte, C. F. The rejection of specific organic compounds by reverse osmosis membranes. *Desalination* **2003**, *158*, 285–294.

(10) Ben-David, A.; Bason, S.; Jopp, J.; Oren, Y.; V Freger., J. Partitioning of organic solutes between water and polyamide layer of RO and NF membranes: Correlation to rejection. *J. Membr. Sci.* **2006**, *281*, 480–490.

(11) Freger, V.; Bason, S. Characterization of ion transport in thin films using electrochemical impedance spectroscopy: I. Principles and theory. *J. Membr. Sci.* **2007**, *302*, 1–9.

(12) Bason, S.; Oren, Y.; Freger, V Characterization of ion transport in thin films using electrochemical impedance spectroscopy: II. Examination of the polyamide layer of RO membranes. *J. Membr. Sci.* **2007**, *302*, 10–19.

(13) Barsoukov, E., Macdonald, J. R., Eds. *Impedance Spectroscopy: Theory, Experiment, and Applications*, 2nd ed.; Wiley Interscience, 2005.

(14) Rubinstein, I.; Rishpon, J.; Gottesfeld, S. An AC-impedance study of electrochemical processes in Nafion-coated electrodes. *J. Electrochem. Soc.* **1986**, *133*, 729.

(15) Bódalo, A.; Gómez, E.; Hidalgo, A. M.; Gómez, M.; Murcia, M. D.; López, I. Nanofiltration membranes to reduce phenol concentration in wastewater. *Desalination* **2009**, *245*, 680–686.

(16) Dražević, E.; Košutić, K.; Fingler, S.; Drevenkar, V. Removal of pesticides from the water and their adsorption on the reverse osmosis membranes of defined porous structure. *Desalin. Water Treat.* **2011**, *30*, 161–170.

(17) Comerton, A. M.; Andrews, R. C.; Bagley, D. M.; Yang, P. Membrane adsorption of endocrine disrupting compounds and pharmaceutically active compounds. *J. Membr. Sci.* **2007**, *303*, 267–277.

(18) Comerton, A. M.; Andrews, R. C.; Bagley, D. M.; Hao, C. The rejection of endocrine disrupting and pharmaceutically active compounds by NF and RO membranes as a function of compound and water matrix properties. *J. Membr. Sci.* **2008**, *313*, 323–335.

(19) Kimura, K.; Toshima, S.; Amy, G.; Watanabe, Y. Rejection of neutral endocrine disrupting compounds (EDCs) and pharmaceutical active compounds (PhACs) by RO membranes. *J. Membr. Sci.* **2004**, *245*, 71–78.

(20) Yoon, Y.; Westerhoff, P.; Snyder, S. A.; Wert, E. C.; Yoon, J. Removal of endocrine disrupting compounds and pharmaceuticals by

nanofiltration and ultrafiltration membranes. *Desalination* **2007**, *202*, 16−23.

(21) Al-Rifai, J. H.; Khabbaz, H.; Schäfer, A. I. Removal of pharmaceuticals and endocrine disrupting compounds in a water recycling process using reverse osmosis systems. *Sep. Purif. Technol.* **2011**, *77* (1), 60−67.

(22) Williams, M. E.; Hestekin, J. A.; Smothers, C. N.; Bhattacharyya, D. Separation of Organic Pollutants by Reverse Osmosis and Nanofiltration Membranes: Mathematical Models and Experimental Verification. *Ind. Eng. Chem. Res.* **1999**, *38* (10), 3683−3695.

(23) Leddy, J; Bard, A. Polymer films on electrodes. Part XII. Chronoamperometric and rotating disc electrode determination of the mechanism of mass transport through poly(vinyl ferrocene) films. *J. Electroanal. Chem.* **1983**, *153*, 223−242.

(24) McCarley, R.; Irene, E.; Murray, R. Permeant molecular sieving with electrochemically prepared 6-nm films of poly(phenylene oxide). *J. Phys. Chem.* **1991**, *95*, 2492.

(25) Kedem, O.; Freger, V. Determination of concentration-dependent transport coefficients in nanofiltration: Defining an optimal set of coefficients. *J. Membr. Sci.* **2008**, *310*, 586−593.

(26) Freger, V. Swelling and morphology of the skin layer of polyamide composite membranes: An Atomic Force Microscopy Study. *Environ. Sci. Technol.* **2004**, *38* (11), 3168−3175.

(27) Ononye, A. I.; McIntosh, A. R.; Bolton, J. R. Mechanism of the Photochemistry of p-Benzoquinone in Aqueous Solutions. 1. Spin Trapping and Flash Photolysis Electron Paramagnetic Resonance Studied. *J. Phys. Chem.* **1986**, *90*, 6266−6270.

(28) Bason, S.; Kedem, O.; Freger, V. Determination of concentration-dependent transport coefficients in nanofiltration: Experimental evaluation of coefficients. *J. Membr. Sci.* **2009**, *326*, 197−204.

(29) Ben-David, A.; Oren, Y.; Freger, V. Thermodynamic factors in partitioning and rejection of organic compounds by polyamide composite membranes. *Environ. Sci. Technol.* **2006**, *40*, 7023−7028.

(30) Freger, V. Diffusion impedance and equivalent circuit of a multilayer film. *Electrochem. Commun.* **2005**, *7*, 957−961.

(31) Freger, V. Nanoscale heterogeneity of the polyamide membranes obtained by interfacial polymerization. *Langmuir* **2003**, *19*, 4791−4797.

(32) Freger, V. Kinetics of film formation by interfacial polycondensation. *Langmuir* **2005**, *21*, 1884−1894.

(33) Bason, S.; Oren, Y.; Freger, V. Ion transport in the polyamide layer of RO membranes: composite membranes and free-standing films. *J. Membr. Sci.* **2011**, *367*, 119−126.

(34) Lonsdale, H. K.; Riley, R. L.; Lyons, C. R.; Carosella, D. P. Transport in composite reverse osmosis membranes. In Bier, M., Ed., *Membrane Processes in Industry and Biomedicine*; Plenum Press: New York, 1971; p 101.

(35) Ramon, G. Z.; Hoek, E. M. V. Transport through composite membranes, part 1: Is there an optimal support membrane?, **2011**, submitted.

(36) Lindau, J.; Jönsson, A. S.; Wimmerstedt, R. The influence of a low-molecular hydrophobic solute on the flux of polysulphone ultrafiltration membranes with different cut-off. *J. Membr. Sci.* **1995**, *106* (1), 9−16.

(37) Bason, S.; Kaufman, Y.; Freger, V. Analysis of ion transport in nanofiltration using phenomenological coefficients and structural characteristics. *J. Phys. Chem. B* **2010**, *114*, 3510−3517.